



# Urease immobilized electrospun PVA/chitosan nanofibers with improved stability and reusability characteristics: an application for removal of urea from artificial blood serum

Nur Kutlu<sup>a</sup>, Yasemin İspirli Doğaç<sup>b</sup>, İlyas Devenci<sup>c</sup>, and Mustafa Teke<sup>a</sup>

<sup>a</sup>Faculty of Science, Chemistry Department, Muğla Sıtkı Koçman University, Muğla, Turkey; <sup>b</sup>Chemistry and Chemical Processing Technology Department, Muğla Vocational School, Muğla Sıtkı Koçman University, Muğla, Turkey; <sup>c</sup>Chemistry and Chemical Processing Technology Department, Technical Sciences Vocational School, Konya Technical University, Konya, Turkey

## ABSTRACT

Electrospun polyvinyl alcohol (PVA)/Chitosan nanofibers were successfully prepared and were used as carriers for the first time in urease immobilization. Also, urease immobilized electrospun PVA/Chitosan nanofibers were applied for the removal of urea from artificial blood serum by recycled reactor. The nanofibers were optimized and synthesized by electrospinning technique according to the operational parameters. The morphology and structure of the nanofibers were characterized by scanning electron microscopy (SEM), attenuated total reflection-Fourier transform infrared spectroscopy (ATR-FTIR) and thermogravimetric analysis (TGA). Urease was immobilized on the nanofibers by adsorption and crosslinking methods. According to immobilization results, nanofiber enhanced urease stability properties like thermal stability, pH stability, and reusability. Urease immobilized electrospun PVA/Chitosan nanofiber protected its activity by 85% after 10 uses and 45% after 20 uses. Urea removal rates of artificial blood serum were as follows: 100% at 1st cycle, 95% at 2nd, 3rd and 4th cycles; 85% at the 5th cycle; 76% at the 6th cycle, and 65% at the last three cycles.

## KEYWORDS

Chitosan; electrospinning; immobilization; nanocomposites; nanofiber; polyvinyl alcohol; urease

## Introduction

Immobilization is the physical or chemical attachment of the soluble enzyme to the insoluble carrier's surface or pores. The main purpose of using immobilization is to allow the enzyme to be easily separated from the reaction medium and to allow reuse. Adsorption, cross-linking, and encapsulation are among the methods used for immobilization. Adsorption is a method that uses weak interactions (Van der Waals forces, ionic and hydrophobic interactions, and hydrogen bonds). Unfortunately, desorption associated with the adsorption of the enzyme is the disadvantage of this method. Cross-linking after adsorption may be an alternative to the solution of this problem. Crosslinking is the process of binding the enzyme to the carrier's surface with a bifunctional agent.<sup>[1–3]</sup> The selection of the carrier is very important for immobilization. Natural and commercial polymers, porous materials, nanorods, nanoparticles, nanofibers have been employed as carrier.<sup>[4–8]</sup> nanocomposites show original chemical and physical properties such as large surface area–volume ratios or high reactivity, so they are studied for potential applications like biomedical, industrial and environmental.<sup>[9–11]</sup> The widely used polymers for nanocomposites are polyvinyl alcohol, poly(ethylene oxide), alginate, chitosan, chitin, epoxy, cellulose acetate,

polyaniline, silk fibroin, polydimethylsiloxane, graphene, collagen, polynorbornene, poly(p-phenylene benzobisoxazole), poly( $\epsilon$ -caprolactone), polyurethane, poly(vinylidene fluoride), polypropylene, gelatin, poly(acrylic acid), polyester, poly( $\beta$ -hydroxybutyrate), fibrinogen etc.<sup>[12–23]</sup>

Nanofibers have a very high potential for enzyme immobilization because of their appropriate functional groups, high porosity, high surface area, the availability of different compositions in the structure, biocompatibility, biodegradability, hydrophilicity (water contact angle), nontoxicity. Nanofibers exhibited a higher enzyme loading ability compared to other immobilization carriers. The enzyme is located in the pores of the nanofibers and three-dimensional structure of the enzyme is protected. Also, the thermal and pH stability of the enzyme is increased.<sup>[24]</sup> Self-assembly, phase separation, template synthesis, and electrospinning are used for synthesizing nanofibers.<sup>[25,26]</sup>

Electrospinning is based on using the high voltage power source by injection polymer solutions on a grounded electrode. The method is suggested as the most suitable method for the production of nanofibers depending on the many offered advantages like cost efficiency, flexibility, mechanical stability and is easy to handle.<sup>[19,27–29]</sup> Electrospun nanofibers may be preferred for immobilized

enzyme, because of their properties as their biocompatibility, biodegradability, hydrophilicity, nontoxicity, besides other features.<sup>[24]</sup> Polyvinyl alcohol (PVA) is a biocompatible, water-soluble, mechanically stable, hydrophilic, chemically stable polymer at high temperature with high dielectric strength. PVA nanocomposites have been studied with many materials such as graphene, starch, montmorillonite, alginate, CdS, TiO<sub>2</sub>, cellulose, cellulose/Ag, Al<sub>2</sub>O<sub>3</sub>, graphene oxide/magnetite, Zn<sup>2+</sup>, etc.<sup>[15,19,23,30–38]</sup> During electrospinning, PVA can reduce conductivity and facilitate the electrospinning process. So, it is a widely used polymer in the electrospinning process.<sup>[39,40]</sup>

Chitosan is a biocompatible polymer that is composed of hydroxyl and amino groups and is derived from deacetylation of chitin. It is also non-toxic, antibacterial and biodegradable. Chitosan shows cationic behavior in acidic solutions due to the presence of amino groups.<sup>[41,42]</sup>

Ureases (urea amidohydrolases, EC 3.5.1.5) catalyze the hydrolysis of urea to ammonia and carbon dioxide. The catalysis reaction is important in the potential practical applications. Urease plays a significant role to remove urea from fruit juice and foods at the food industry, to accelerate the hydrolysis of urea at the agricultural fertilizer, to remove urea from blood at the artificial kidney studies, to calculate the amount of urea in biological fluids, to remove urea in wastewater.<sup>[43]</sup>

In this present study, PVA/Chitosan nanofibers were prepared using electrospinning technique. This study presents not only the characterization of PVA/Chitosan nanofibers but also the usability of the nanofibers for urease immobilization, the increase of enzyme's stability properties and a recycled reactor application for removal of urea from artificial blood serum. So, a model for the usability of PVA/chitosan nanofibers for enzyme immobilization is presented. In light of this work, it is thought that PVA/chitosan nanofiber structures can be used for different applications, especially drug delivery systems.

## Experimental

### Materials

Polyvinyl alcohol (PVA) (99% hydrolyzed;  $M_w = 130$  kDa), Chitosan, Triton X-100, Jack bean urease (Type III), urea, glutaraldehyde (GA) and all other reagents were purchased from Sigma-Aldrich.

### Preparation of PVA/chitosan nanofibers by electrospinning method

Electrospun PVA/Chitosan nanofibers were used by modifying our previous works.<sup>[12,23]</sup> By modifying the method, proper formation of the tailor cone on the electrode of the polymer mixture, the stability of the system at the needle end, the stability of the system, easy separation of the resulting fibers from the collector, the mechanical strength of the fibers and the drop of polymer mixture on the collector in the form of droplets were achieved. Aqueous electrospinning solutions of PVA/Chitosan with different concentrations

(6–8% for PVA; 0.5–1% for Chitosan, with a ratio of 50:50, were prepared by stirring for 6 hr. In the end, 1% (v/v) Triton X-100 was added to the electrospinning solution and stirred for 2 hr. The solution was placed into a syringe. A syringe pump (New Era Pump Systems Inc., Farmingdale, NY) should be added to the electrospinning system (Inovenso nanospinner, Inovenso Inc., Boston, MA). Voltage (13–16 kV), flow rate (0.2–0.6 mL/hr), and needle tip-collector distance (16–20 cm) were used as the electrospinning system parameters.

### Cross-linking of electrospun PVA/chitosan nanofibers

PVA/Chitosan nanofibers can dissolve in water. So, this type of nanofiber must be crosslinked before any applications. Crosslinking with GA, in which the hydroxyl groups of PVA and the aldehyde groups of GA are reacted in the presence of a strong acid, is a high yielding reaction.<sup>[12,23]</sup> So, the electrospun PVA/Chitosan nanofibers were cross-linked by non-aqueous 1.4% (v/v) GA solution containing 28 mL of 25% GA, 2 mL of 37% HCl, and 470 mL acetone at room temperature for 24 hr to obtain water-insoluble nanofibers. Then, the cross-linked nanofibers were washed in distilled water for several times.

### Characterization of electrospun nanofibers

The surface morphology of electrospun PVA/Chitosan nanofibers was studied by scanning electron microscopy (SEM) using JEOL JSM 7600 F model (JEOL, Akishima, Japan). Surface groups and chemical structure of the electrospun nanofibers were analyzed by using attenuated total reflection-Fourier transform infrared spectroscopy (ATR-FTIR) (Thermo Scientific Nicolet iS-5 ATR/FTIR Spectrometer) at a high resolution between 350 and 4000 cm<sup>-1</sup>. Thermal analysis of raw polymers and obtained nanofibers were performed using Perkin Elmer TGA 4000 (thermo-gravimetric analyzer) at a constant heating rate of 20 °C/min at 50–650 °C.

### Using electrospun PVA/chitosan nanofibers for urease immobilization

The electrospun nanofibers were used for urease immobilization as a carrier. Adsorption and then cross-linking methods were chosen for the immobilization process. The known amount of PVA/Chitosan nanofiber (5, 7.5, 10, 12.5, 15, and 20 mg) was added to 1 mL urease solution (0.5, 0.75, 1, 1.5, and 2 mg/mL, respectively) and stirred at the room temperature for the fixed times (5–75 min). Then, different concentrations of GA (1, 2, 3, and 4% v/v) were added to the solution and stirred for 15 min. Finally, urease immobilized PVA/Chitosan nanofibers were washed with distilled water several times.

### Urease activity assay

Urease activity was determined by the Berthelot method.<sup>[44]</sup> 1.94 mL (50.0 mM; pH 7.0) phosphate buffer, 0.1 mM 10  $\mu$ L

of urea and 50  $\mu\text{L}$  urease enzyme solution were added to tube. The mixture was incubated for 10 min at room temperature with stirring. Phenol reagent (500  $\mu\text{L}$ ) and hypochlorite reagent (500  $\mu\text{L}$ ) were added to the tube and incubated for 5 min at 50 °C. The activity of urease was measured spectrophotometrically at 630 nm. The definition of one unit urease activity is the hydrolysis of 1  $\mu\text{mol}$  urea per minute at 25 °C and pH 7.0.

### Determination of enzymatic properties of urease immobilized PVA/chitosan nanofibers

The temperature was varied between 20 and 55 °C during the activity assay for optimum temperature determination. For determination of the thermal stabilities, the free urease and urease immobilized PVA/Chitosan were kept at 50 °C and 60 °C for 110 min by measurement of the urease activities every after 10 min.

To detect the optimum pH of free and immobilized urease, the enzymatic activity was measured at different pHs from 3.0 to 10.0. The free and urease immobilized nanofiber were kept at varying pH, in the range 3.0–10.0, for 1 hr to compare the pH stabilities.

Reusability of the urease immobilized electrospun PVA/Chitosan nanofiber was assessed by repeating enzyme assay 32 times under standard assay conditions. After each cycle, immobilized urease was separated from supernatant and washed with water three times and the reaction medium was changed with fresh urea solution.

The enzymatic activity assays of free and immobilized urease were studied for different concentrations (0.023–0.23 mM) of urea solutions under activity assay conditions to compared the Michaelis–Menten constant ( $K_m$ ) and the maximum velocity ( $V_{max}$ ). The kinetic parameters were calculated by Lineweaver–Burk plots based on the Michaelis–Menten equation. The descriptions of Michaelis–Menten equation and Lineweaver–Burk plots were given Eqs. (1) and (2) respectively.

$$v = \frac{V_{max} \cdot [S]}{K_m + [S]} \quad (1)$$

$$\frac{1}{V} = \frac{K_m}{V_{max}} \times \frac{1}{[S]} + \frac{1}{V_{max}} \quad (2)$$

### Recycled reactor design with urease immobilized PVA/chitosan nanofibers for urea removal from artificial blood serum

Recycled reactor enzyme systems ensure optimum reaction conditions remain constant and control of the reaction. In order to investigate the urea removal performance from artificial blood serum of urease immobilized PVA/Chitosan nanofibers were used recycled reactor system (enzyme column, peristaltic pump, and serum reservoir). In the double-walled enzyme column, urease immobilized PVA/Chitosan nanofibers were used and water was continuously passed through the outer wall at 37 °C to create a constant

temperature. The serum sample content was adjusted to 2.5 mM urea, 4.7 mM D(+) glucose, 0.1% albumin, 145 mM NaCl, 5 mM  $\text{CaCl}_2$ , 4.5 mM KCl, 1.6 mM  $\text{MgCl}_2$ . Samples were taken from the serum reservoir at specific intervals to determine the performance of each cycle.

## Results and discussion

### Optimization and characterization of electrospun PVA/chitosan nanofibers

In the literature, it is pointed out that polymers such as alginate and chitosan can not form nanofiber by electrospinning alone, and that they can form composite fibers together with the polymer such as water-soluble PVA.<sup>[45,46]</sup> The factors which are affecting the formation of smooth fibers, the voltage applied parametrically, the distance between the needle and the collector, the polymer concentration and composition, the flow rate of the polymer mixture. In this study, all of these parameters were investigated for electrospun PVA/Chitosan nanofibers. The results are given in Table 1. For the PVA/Chitosan nanofibers, 6% PVA concentration, 1% Chitosan concentration, 16 kV application voltage, 20 cm needle-collector distance and 0.2 mL/hr polymer flow rate were determined as optimum conditions. Following this step, SEM, FTIR, and thermogravimetric analysis (TGA) characterization of the nanofibers prepared with the most appropriate parameters were performed.

SEM is a very powerful technology to determine the morphology of nanomaterials. SEM photos of raw PVA/Chitosan nanofibers and cross-linked PVA/Chitosan nanofibers are shown in Figures 1 and 2. In Figure 1, nanofibers were randomly positioned, smooth, rounded. Their average diameters were around 140–220 nm. After cross-linking, the photos given in Figure 2 indicated that the nanofibers continued to maintain smooth and rounded lines. Also, their average diameters are decreased (100–210 nm). Nanofiber structures and diameters are also consistent with similar studies in the literature.<sup>[22,47,48]</sup> SEM images of urease immobilized PVA/Chitosan nanofibers were given in Figure 3. After immobilization, the structures of the nanofibers did not change and the average diameters were around 200–250 nm. The reason for the increase in diameter after immobilization can be explained by the amount of cross-linked enzyme on the surface.

The ATR-FTIR spectra of PVA, Chitosan and PVA/Chitosan nanofiber structure are shown in Figure 4. Two peaks are observed in the spectrum of PVA between 3000–3600  $\text{cm}^{-1}$  and 2850–3000  $\text{cm}^{-1}$ , respectively in the free alcohol groups –OH vibration band and C–H peak. Chitosan structure of the spectrum between 3693  $\text{cm}^{-1}$  and 2996  $\text{cm}^{-1}$  with –OH stress peaks along with N–H strain peaks are seen. In this range, the –OH strain peaks cover the N–H tensile peaks. The peak found at 2875  $\text{cm}^{-1}$  indicates the lithography where C–H stress is caused. In addition, tensile vibrations of these structures are seen in 1372  $\text{cm}^{-1}$  and 1429  $\text{cm}^{-1}$  in both the structures of the two polymers, which are more prominent in the structure of PVA. Chitosan structure specific to the peak amide



**Table 1.** Preparation parameters of PVA/Chitosan nanofiber and observations.

Chitosan concentration (%)	PVA concentration (%)	Application voltage (kV)	Needle-collector distance (cm)	Polymer flow rate (mL/hr)	Observations*
0.5	6	13	16	0.3	–
0.5	6	15	17	0.5	–
0.5	6	15	17	0.5	+
0.5	6	16	20	0.5	++
0.5	7	15	20	0.3	++
0.5	7	15	18	0.5	–
0.5	7	15	19	0.5	–
0.5	7	16	14	0.3	++
0.5	8	15	20	0.3	++
0.5	8	15	20	0.5	–
1	6	13	18	0.2	++
1	6	16	20	0.2	++++
1	6	15	20	0.3	–
1	6	16	20	0.5	++–
1	7	13	18	0.6	+–
1	7	15	18	0.5	–
1	7	15	20	0.5	–
1	7	16	20	0.6	++

\*Positive (+) parameters: Proper formation of the tailor cone on the electrode of the polymer mixture. The stability of the system at the needle end. Easy separation of the resulting fibers from the collector. The mechanical strength of the fibers. Negative (–) parameters: The drop of polymer mixture on the collector in the form of droplets. Note. 1% Triton X-100 was added to all solutions.

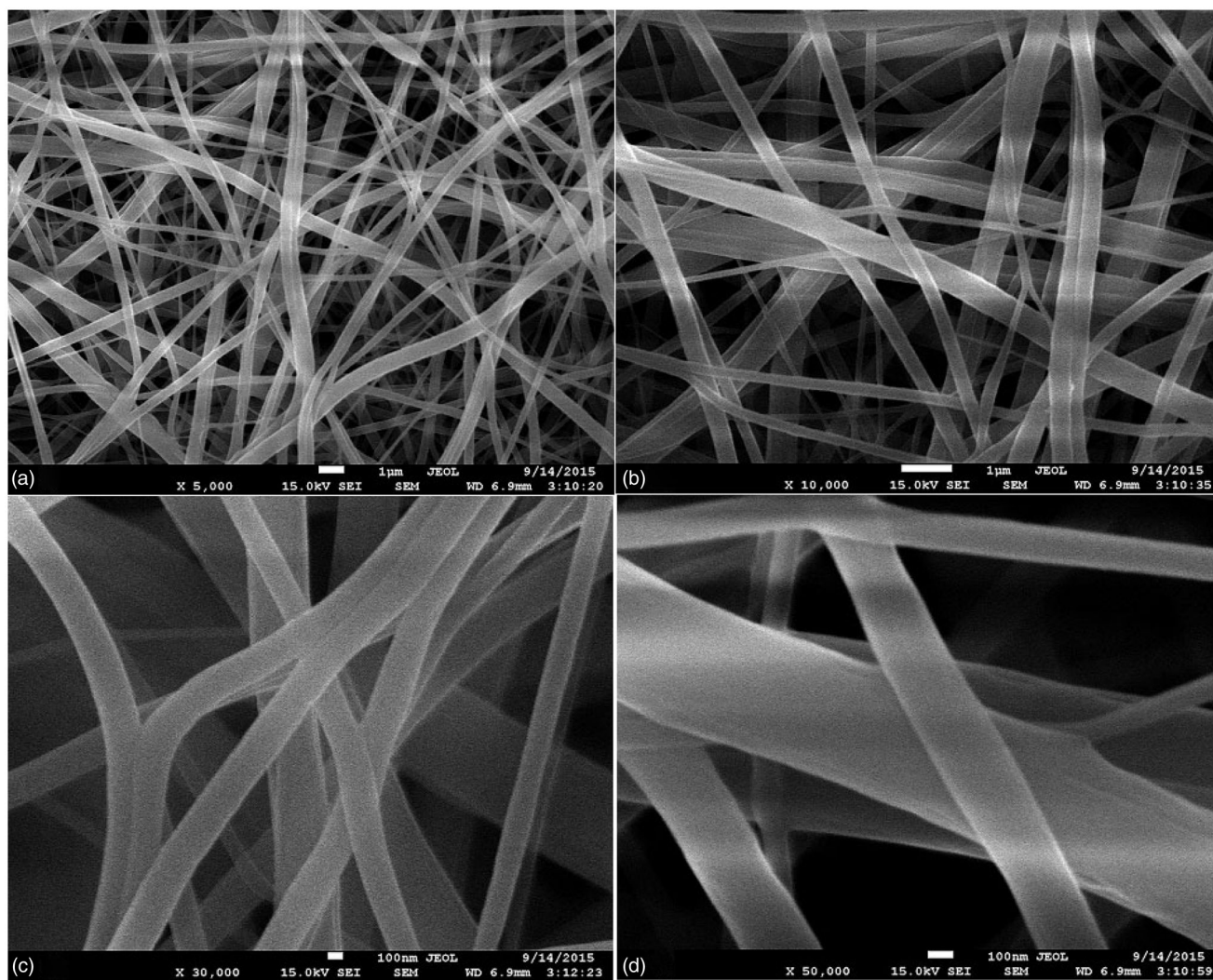


**Figure 1.** SEM photos of PVA/Chitosan nanofibers: (a) 5000 $\times$ , (b) 10,000 $\times$ , (c) 30,000 $\times$ , and (d) 50,000 $\times$  upgrades. (Optimum nanofiber synthesis conditions: 6% PVA concentration, 1% Chitosan concentration, 50:50 PVA/Chitosan ratio, 16 kV application voltage, 20 cm needle-collector distance, 0.2 mL/hr polymer injection rate).

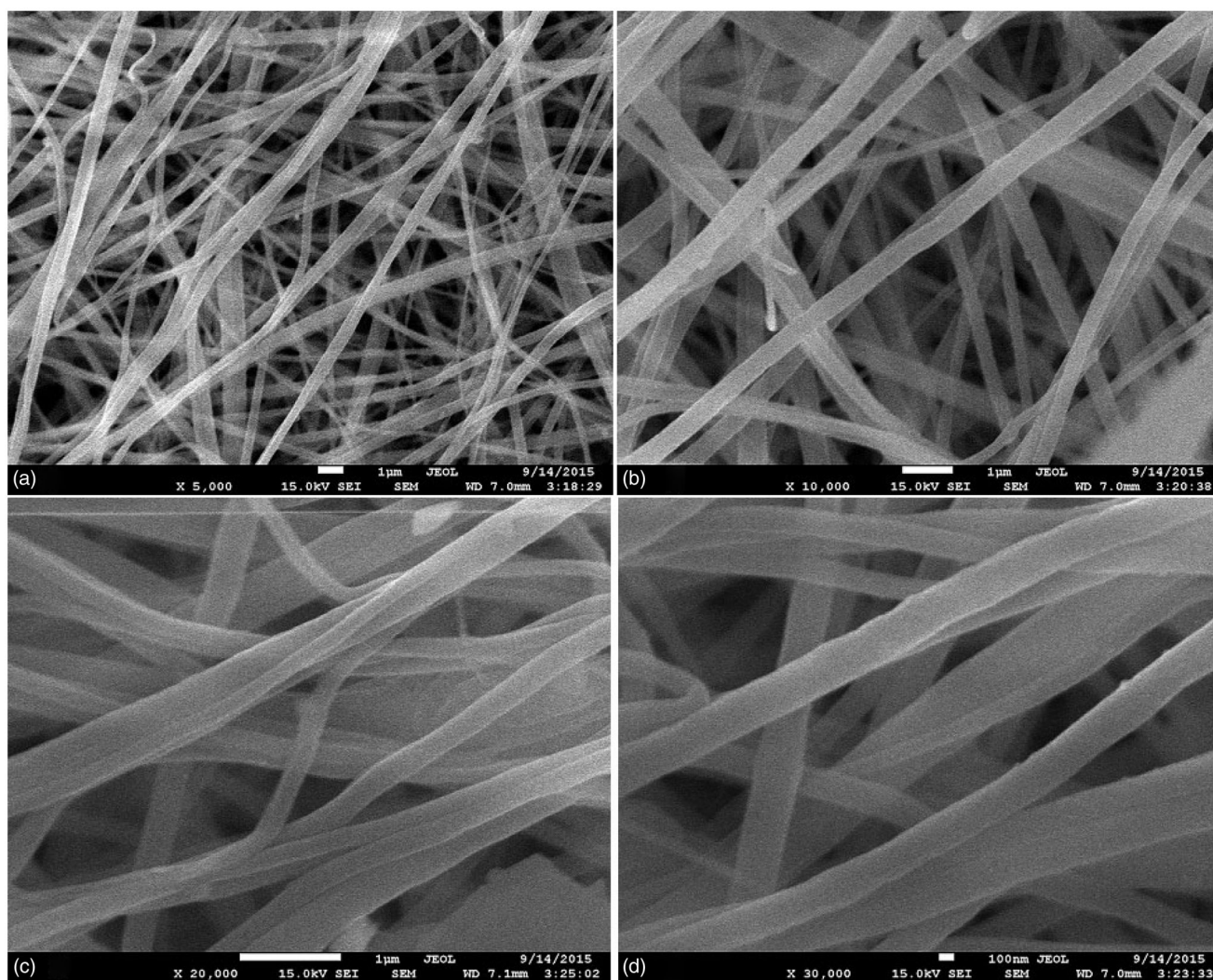


**Figure 2.** SEM photos of cross-linked PVA/Chitosan nanofibers, (a) 5000 $\times$ , (b) 10,000 $\times$ , (c) 20,000 $\times$ , and (d) 30,000 $\times$ , with magnifications. (Optimum nanofiber synthesis conditions: 6% PVA concentration, 1% Chitosan concentration, 50%: 50 PVA/Chitosan ratio, 16 kV application voltage, 20 cm needle-collector distance, 0.2 mL/hr polymer injection rate; anhydrous glutaraldehyde solution, 2 hr incubation).

(CONHR) group of  $1636\text{ cm}^{-1}$  depending on the vibration ( $\text{C}=\text{O}$ ) vibrations and the peak seen in  $1589\text{ cm}^{-1}$  protonated amine groups is stated in the literature.<sup>[22,48]</sup> In the ATR-FTIR spectrum of PVA/Chitosan Nanofiber structure, the peaks of the raw materials of the polymers were preserved although there were very few shifts.

Thermogravimetric (TG) and differential thermogravimetric (DTG) curves of PVA, Chitosan and composite PVA/Chitosan nanofiber structures are shown in Figure 5. Considering the TG and DTG curves obtained by the thermal gravimetric analysis of the Chitosan, it is seen that the decrease in the mass occurs in three stages. It is seen that the decrease in the mass caused by the removal of water from the structure of the Chitosan below  $190^\circ\text{C}$  from the structure is due to thermal degradation in the glucosamine structure of 45% between  $256\text{--}363^\circ\text{C}$  and the charring at  $363\text{--}600^\circ\text{C}$ . At the end of thermal degradation at  $600^\circ\text{C}$ , the residual amount of Chitosan was found to be 31%. Considering the DTG curve of Chitosan, the maximum rate

of degradation was  $317^\circ\text{C}$ . In Figure 5, three-step mass reduction was observed in the TG curve obtained for the PVA structure. In step 1, it is thought that 4% reduction below  $190^\circ\text{C}$  for the raw PVA structure is caused by the removal of water due to the structure. In the second stage, with a sharp decrease between  $265$  and  $325^\circ\text{C}$ , 70% of the polymer mass was removed from the structure. The decrease in the mass is characterized by  $\text{H}_2\text{O}$  elimination and chain stripping reactions in this stage.<sup>[49]</sup> In phase 3, 15% of the first mass between  $415\text{--}500^\circ\text{C}$  moved away from the structure. It is also suggested in the literature that the decrease in mass is due to  $\text{H}_2$  elimination reaction.<sup>[49,50]</sup> The amount of ash residue of the structure after the experiment was found to be 4%. The DTG curve shows 2 peaks at  $293$  and  $460^\circ\text{C}$  for the raw PVA. These peaks show the temperatures at which the maximum decomposition of steps 2 and 3, respectively, occur. TG and DTG curves of PVA/Chitosan nanofiber structure, the raw states of the two polymers differ slightly from TG and DTG curves. Interactions between



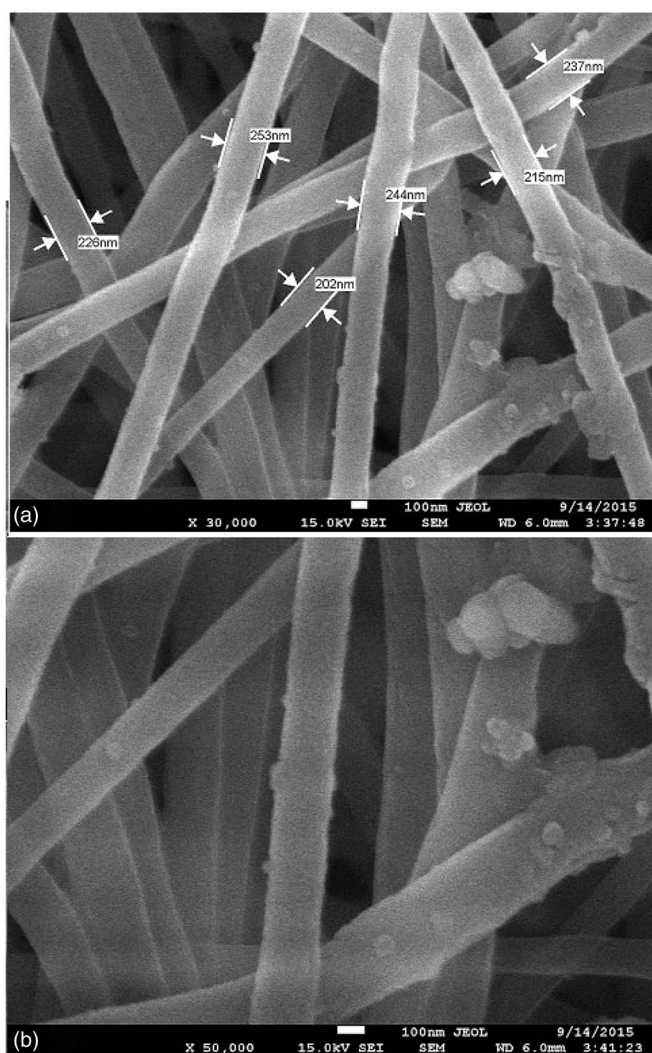


**Figure 3.** SEM photos of urease immobilized cross-linked PVA/Chitosan nanofibers, (a) 30,000 $\times$ , and (b) 50,000 $\times$  with magnifications.

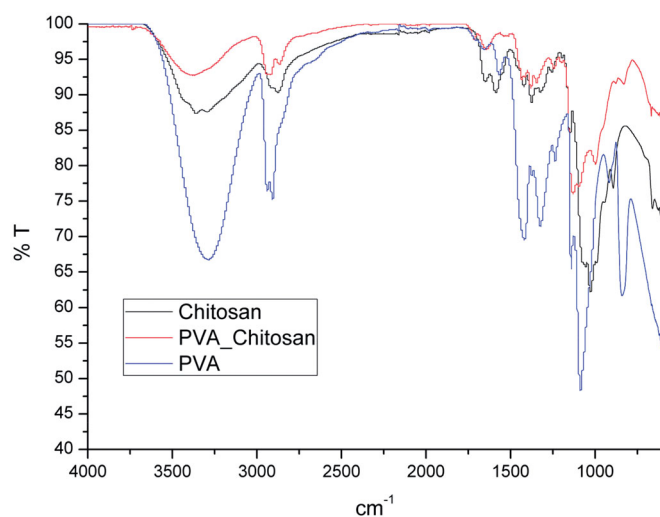


**Figure 4.** Raw Chitosan, raw PVA and PVA/Chitosan nanofiber ATR-FTIR Spectra.

polymers and differences in the textural structure may have caused different thermal decomposition curves. The PVA/Chitosan nanofiber structure showed a 5% mass reduction

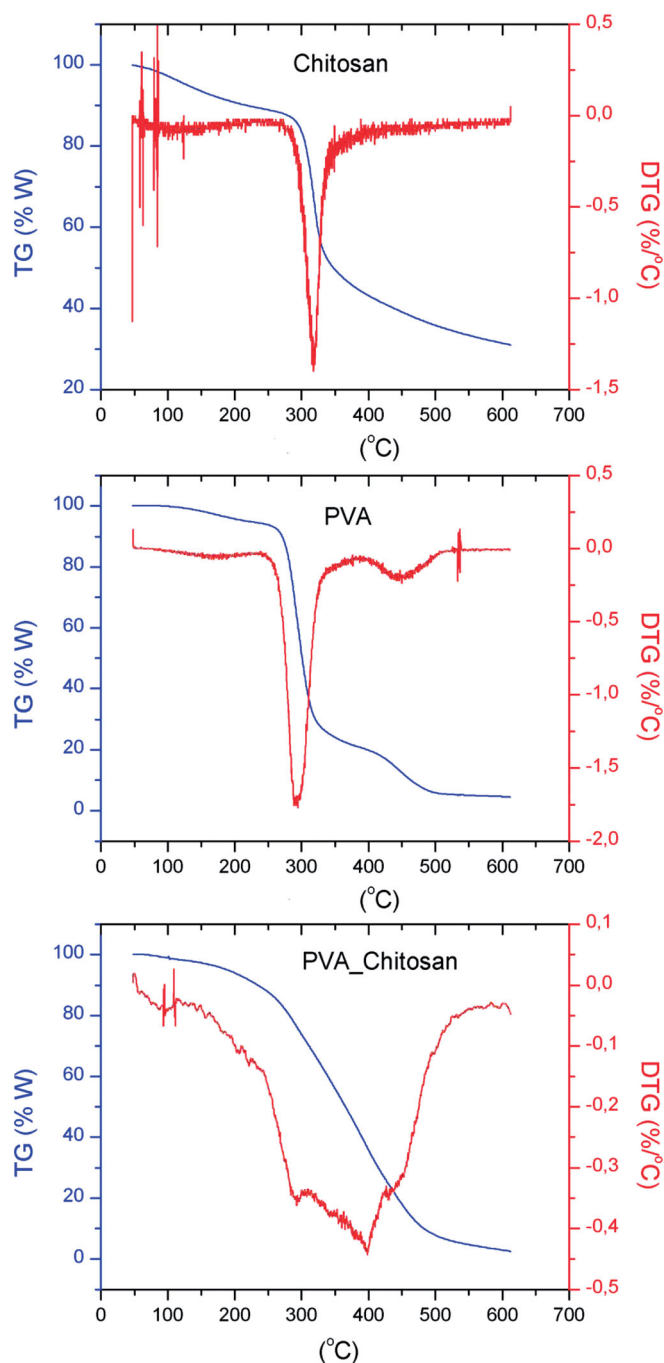


**Figure 5.** Raw Chitosan, raw PVA and PVA/Chitosan nanofiber TGA and DTG curves.

of up to 190 $^{\circ}$ C in the TG curve. This reduction is thought to be due to the removal of physically bound water as in other raw polymers. After this stage, a constant decrease in the mass between 210–510 $^{\circ}$ C was observed. This reduction was softer compared to other polymers. Between 210–510 $^{\circ}$ C, 88% of the structure is degraded compared to the initial mass. This may be due to the hydrogen bond and glutaraldehyde cross-linking between the  $-\text{NH}_2$  and  $-\text{OH}$  groups in the structure of Chitosan and PVA which make up the nanofiber structure. This is more evident in DTG curves. The maximum decay temperature for Chitosan and PVA is 317 and 293 $^{\circ}$ C respectively, and the maximum decay temperature for PVA/Chitosan nanofiber structure is 397 $^{\circ}$ C. The

**Table 2.** The activity and specific activity values of free and immobilized ureases.

Amount of the urease (mg/mL)	Free urease		Immobilized urease	
	Activity (U)	Specific activity (U/mg protein)	Activity (U)	Specific activity (U/mg protein)
0.5	0.152 ± 0.008	0.481 ± 0.024	0.118 ± 0.006	0.383 ± 0.019
<b>0.75</b>	0.210 ± 0.011	0.585 ± 0.029	0.141 ± 0.007	<b>0.437 ± 0.022</b>
1	0.218 ± 0.011	0.422 ± 0.021	0.159 ± 0.008	0.336 ± 0.017
1.5	0.232 ± 0.012	0.306 ± 0.015	0.160 ± 0.008	0.216 ± 0.011
2	0.234 ± 0.012	0.238 ± 0.012	0.162 ± 0.008	0.171 ± 0.009

Those shown in bold are the values for which optimum activity is achieved.

amount of ash residue for the PVA/Chitosan nanofiber structure was found as 2.6% at the end of the analysis.

### Optimization of urease immobilization to electrospun PVA/chitosan nanofibers

Firstly, urease was adsorbed on PVA/Chitosan nanofibers and then was cross-linked by glutaraldehyde. Optimization parameters as amount of urease, amount of nanofiber, adsorption time, glutaraldehyde concentration were investigated.

The results of the optimum amount of urease are given in Table 2. According to the results the optimum amount of enzyme for PVA/Chitosan nanofibers was determined as 0.75 mg/mL. It is probably because the amount of PVA/Chitosan nanofiber was not enough for urease immobilization. Also, this may result from the multi-adsorption of urease on surface of the nanofiber. The effects of enzyme concentration on urease immobilization in various nanomaterials were investigated in the literature. In a study conducted on urease immobilization on aluminum oxide membrane, urease enzyme concentration was used as 4 mg/mL.<sup>[51]</sup> The enzyme concentration of urease enzyme was used as 1.02 mg/mL on the glycidyl methacrylate-alginate copolymer.<sup>[52]</sup> In a study of urease enzyme immobilization on alkyl modified nanoporous silica, 0.3 mg/mL enzyme was used.<sup>[53]</sup> 5 mg/mL urease was used for ethylcellulose polymethacrylic acid polymer.<sup>[54]</sup> In the urease immobilization study of TiO<sub>2</sub> and TiO<sub>2</sub>/Chitosan beads, the optimum amount of urease was used as 1 mg/mL.<sup>[55]</sup> In another study on immobilization of biocompatible polymeric-magnetic nanoparticle composites, the optimum amount of urease was found to be 1.5 mg/mL.<sup>[56]</sup>

The optimum amount of nanofiber (when the urease amount was kept constant at 0.75 mg/mL) was determined as 15 mg. At the amounts below the optimal value, all of the enzyme molecules may not immobilized, because there are not enough carriers in the medium. At the amounts above the optimum value, the high amount of nanofiber can cause steric hindrance during immobilized enzyme-substrate interactions. In a study about the urease immobilized N-phosphonomethyliminodiacetic acid-modified Fe<sub>3</sub>O<sub>4</sub> nanomagnetic particles, 50 mg magnetic particle was used for 1.25 mg/mL urease amount.<sup>[57]</sup> Five milligrams of nanofiber was used for the enzyme immobilization on electroexpanded poly (acrylonitrile-co-2-hydroxyethyl methacrylate) nanofibers<sup>[58]</sup> and cellulose nanofibers.<sup>[59]</sup> In a study conducted in 2017, electrospun polyethylene oxide/alginate and polyvinyl alcohol/alginate nanofibers were used for

enzyme immobilization and the optimum amount of nanofiber was found to be 7.5 and 10 mg, respectively.<sup>[12]</sup>

The optimum adsorption time was found as 30 min. This result can be explained as follows: Generally, the adsorption time depends on the number of functional groups on the surface of the carrier and the number of groups on the surface of the enzyme and the non-covalent bonding strength between these groups. So, the surface of the nanofiber reached saturation of urease molecules at 30 min, and the surface desorption was started for longer than 30 min. Also, due to the amino acids in the structure of the immobilized enzyme, the interest of the enzyme in the nanofiber causes a change in the adsorption time. In a study, the adsorption time for the urease immobilized on copper chelated-Eupergit C beads was determined as 3 hr.<sup>[60]</sup> In the other study, electrospun polyethylene oxide/alginate and polyvinyl alcohol/alginate nanofibers were used for enzyme immobilization and were found to be 20 min as optimum adsorption time.<sup>[12]</sup>

2% (v/v) was found as the optimum glutaraldehyde concentration value. It was determined that the activity in the amounts above 2% GA decreased. It can be thought that the conformational change caused by glutaraldehyde addition to the active center of the enzyme may cause this situation. In the studies; cellulosic cotton fibers were applied to urease immobilization using a concentration of 10% (v/v) glutaraldehyde.<sup>[61]</sup> 0.1% (v/v) GA concentration during urease immobilization was applied to the functionalized carbon nanotubes with polypyrrole.<sup>[62]</sup> In another study, when we performed catalase immobilization on Fe<sub>3</sub>O<sub>4</sub> and Fe(NiFe)O<sub>4</sub> type magnetic nanoparticles, the optimum activity was reached when glutaraldehyde concentration was 3% (v/v).<sup>[63]</sup> Polyaniline grafted magnetic poly (2-hydroxyethylmethacrylate-glycidylmethacrylate) hydrogels were used for glucoamylase immobilization and 0.5% (v/v) glutaraldehyde concentration was the optimum value.<sup>[64]</sup> Urease immobilization was performed on TiO<sub>2</sub> beads and optimum glutaraldehyde concentration was determined as 2% (v/v).<sup>[65]</sup> Electrospun polyethylene oxide/alginate and polyvinyl alcohol/alginate nanofibers were used for enzyme immobilization and the optimum glutaraldehyde concentration was found to be 2%.<sup>[12]</sup>

### Characterization of urease immobilization to electrospun PVA/chitosan nanofibers

#### Temperature properties

The temperature increase usually has a positive effect on reaction rates. However, this effect shows a positive tendency to the optimum temperature due to the protein

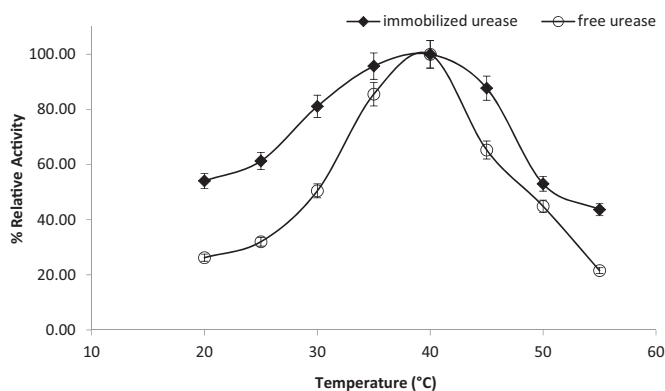


**Figure 6.** Optimum temperature curves of free and urease immobilized PVA/Chitosan nanofibres (0.75 mg/mL urease amount, 15 mg fiber amount, 30 min adsorption time, 20  $\mu$ L GA, pH 7 phosphate buffer).

structure of the enzymes. When the optimum temperature is exceeded, the enzymes are denatured and their activities may be reduced. The optimum temperature is the temperature at which the enzyme has the highest activity and the intermolecular interactions are highest. As shown in Figure 6, the optimum temperature was found to be 40 °C for both the immobilized and the free urease. There is no change in the optimum temperature of the free enzyme and the immobilized enzyme. At other temperatures the activity values of the immobilized enzyme are higher than the free enzyme, so the immobilized urease temperature profile is wider. The reason for this is that the porous structure of the PVA/Chitosan nanofibers and the netting formed on the nanofibers' surface can contribute to maintaining the stability and activity of the enzyme at high temperatures.

In a study about urease immobilized poly (2-hydroxyethyl methacrylate-co-N-methacryloyl-L-histidinemethylester), the optimum activity was observed 45 °C for free urease and 50 °C for immobilized urease.<sup>[65]</sup> In another study, when the optimum temperature of free urease was found at 37 °C, the value was slipped to 50 °C for urease immobilized on commercial membrane.<sup>[66]</sup> In another study; when the optimum temperature for free urease was 55 °C, it was observed 60 °C for urease immobilized on copper chelated Eupergit C beads.<sup>[60]</sup> In another study about urease immobilized on cellulosic cotton fibers, 5 °C shift was observed.<sup>[61]</sup> The optimum temperature value of free urease was observed at 35 °C, while 30 °C for free urease.<sup>[55]</sup> In a study on urease immobilized alginate beads, the optimum temperature of both immobilized and free urease was reported to be 40 °C.<sup>[66]</sup> In the study, which applied urease immobilized Chitosan/magnetic composite beads, the optimum temperature for both free and immobilized enzyme was found to be 35 °C.<sup>[56]</sup>

One of the important factors that play a role in the activity of enzymes is thermal stability. The ability of enzymes to maintain their stability and activity in a wide temperature range allows an industrial preference. In order to determine the thermal stability of immobilized urease and free urease to PVA/Chitosan nanofibers, studies were performed at 50 °C and 60 °C. The results were given in Figure 7. The urease immobilized to PVA/Chitosan nanofibers still retained

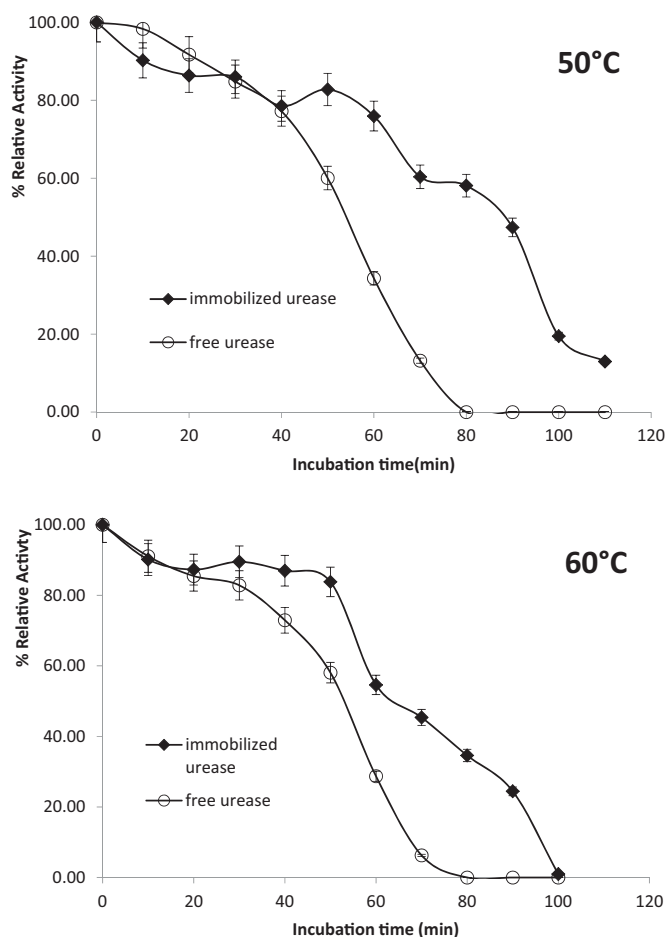


**Figure 7.** Thermal stability curves of free and urease immobilized PVA/Chitosan nanofibres (0.75 mg/mL urease amount, 15 mg nanofiber amount, 30 min adsorption time, 20  $\mu$ L GA).

activity at a rate of 58.11% after 80 min incubation at 50 °C, while the free enzyme showed no activity. At 60 °C, the immobilized urease retained its activity by 34.6% after 80 min incubation while the free urease showed no inactivity and was denatured. The reason for the immobilized enzyme maintained its stability was similar to the expansion in the optimum temperature profile. Groups in the structure of the fibers may be prevented from denaturing the center of the enzyme at high temperatures. Furthermore, the energy necessary to break the stable bonds formed between the fiber and the enzyme increased the stability.

In a study on urease immobilized on arylamine glass beads showed 80% activity at 70 °C, while free one showed 30% activity.<sup>[67]</sup> The activity of free urease after incubation at 60 °C was 75%, whereas the activity of the urease immobilized to the carrier consisting of PMIDA-modified Fe<sub>3</sub>O<sub>4</sub> magnetic particles was found 90% under the same conditions.<sup>[57]</sup> In another study about urease immobilized on TiO<sub>2</sub> beads, immobilized urease enzyme was maintained at 45% at 60 °C, while the activity of free urease was found to be 10%.<sup>[55]</sup>

#### pH properties

The activity of the enzymes may vary depending on the pH of the medium. The enzymes are not very resistant to



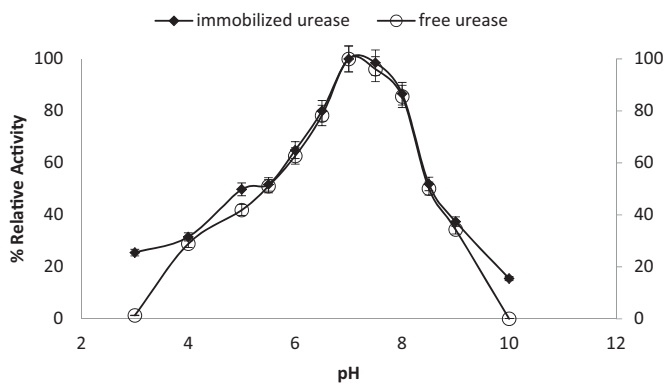


**Figure 8.** Optimum pH curves free and urease immobilized PVA/Chitosan nanofibers (0.75 mg/mL urease amount, 15 mg fiber amount, 30 min adsorption time, 20  $\mu$ L GA).

extremely acidic and basic environments. Changing the pH of the medium causes a change in the ionic state of the enzyme and substrate. At very low or high pH, the enzymes may be denatured and as a result, they may lose their activity. In order to observe the effect of pH on the activity for immobilized urease and free urease enzyme, activity measurements were made by changing the pH between 3.0–10.0 and the calculated relative activity values were given in Figure 8.

In optimum pH studies, a similar profile was observed for both free enzyme and immobilized enzyme. However, no activity was observed in the free enzyme at pH 3 and pH 10, while the immobilized enzyme maintained 20% activity. The activity was maintained in low and high pH environments due to the binding of the functional groups of the enzyme to the nanofiber's functional groups during immobilization. The most important effect is the PVA/Chitosan composite nanofiber. -OH groups of both PVA and Chitosan can be thought to provide partial protection to the enzyme with the effect of buffering the microenvironment of the enzyme in high basic environments. For the same reason, the -NH<sub>2</sub> groups of Chitosan can be considered to provide protection to the immobilized enzyme, although it is buffering effect on the microenvironment of the enzyme in high acidic environments.

In a study, the optimum pH for urease-immobilized PMIDA-modified Fe<sub>3</sub>O<sub>4</sub> magnetic particles was 8.0, whereas the optimum pH for free urease enzyme was 7.0.<sup>[49]</sup> In another study, the optimum pH of the free urease enzyme was 7.4 and the optimum pH of the urease enzyme which was immobilized to a commercial membrane changed to 7.0.<sup>[66]</sup> The urease enzyme was immobilized to copper chelated-Eupergit C beads and optimum pH shifted to 8.0.<sup>[60]</sup> In another study about urease immobilized on cellulosic cotton fibers; optimum pH of immobilized urease has been reported to shift from 6.5 to 7.0.<sup>[61]</sup> In another study that immobilized urease on TiO<sub>2</sub> beads, it was observed that the optimum pH of immobilized urease showed shifts compare to the free enzyme, and the immobilized enzyme showed more activity in the acidic region.<sup>[55]</sup> In some studies, optimum pH profiles of immobilized and free enzyme can be similar. For example, in one study, urease enzyme was

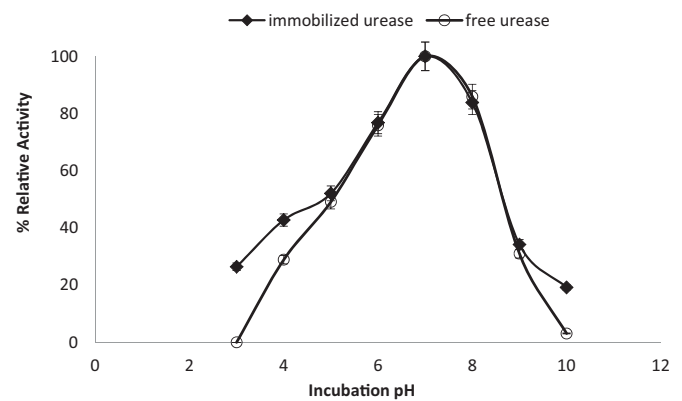


**Figure 9.** pH stability curves of free and urease immobilized PVA/Chitosan nanofibers (0.75 mg/mL urease amount, 15 mg fiber amount, 30 min adsorption time, 20  $\mu$ L GA).

immobilized on arylamine glass beads and showed similar pH profile with free one.<sup>[67]</sup>

In order to determine pH stability, the urease enzyme and free urease enzyme immobilized to PVA/Chitosan nanofibers were incubated in buffers in the range 3.0–10.0 for 1 hr. The results of pH stability were presented in Figure 9.

Both the immobilized and free urease enzyme showed similar relative activities in the range of pH 5.0–9.0. However, the free enzyme does not exhibit any activity between pH 3.0 and 10.0, while the immobilized enzyme maintained the 20% activity under the same conditions. The reason that the immobilized enzyme protected some of its activity in very acidic and very basic medium is the binding of the enzyme to the nanofibers by the hydroxyl, amino and carbonyl groups and the carrier surrounded the microenvironment of the enzyme. In a study, for urease immobilized aryl-glass and alkyl-glass, it has been shown that stability increases in acidic and basic environments.<sup>[68]</sup> When the pH stability of the urease immobilized polyacrylonitrile-Chitosan composite membrane was compared with the free one, no change was observed.<sup>[69]</sup> In the other study, at pH 3.0 and 8.0, free urease lost all its activity, while urease immobilized TiO<sub>2</sub> beads retained 60% activity.<sup>[55]</sup>

### Kinetic parameters

The changes in the 3D structure, the steric barriers and the diffusion limitation, the change of the micro-environment of the enzyme are the disadvantages that may occur during immobilization. In such cases, differences in the kinetic behavior of the enzyme may also occur. In order to observe this change, the kinetic parameters of free urease and urease immobilized PVA/Chitosan nanofibers were determined using the Lineweaver-Burk approach at the 0.023–0.23 mM urea range under optimum activity conditions and  $K_m$  and  $V_{max}$  values were given in Table 3. The immobilized enzyme showed a small increase at  $K_m$  and a small decrease in  $V_{max}$  when compared to the free enzyme. When these results are evaluated thermodynamically, it can be said that the immobilized urease requires a little more free energy to form the transition state. This means that the conformation of the

active site of the immobilized enzyme continues to maintain the shape of the transition state. This situation is often seen for immobilization studies in the literature. In a study, urease was immobilized on the 2-hydroxyethylmethacrylate/itaconic acid copolymer and  $K_m$  value increased from 3.3 mM to 6.25 mM and  $V_{max}$  value decreased from 526.8 U/mg protein to 216.8 U/mg protein compare with free one.<sup>[70]</sup> In another study, urease immobilized on the polyaniline membrane and the  $K_m$  value was found to be 1.35 fold higher than the free enzyme.<sup>[71]</sup>

### Reusability

The greatest advantage of the immobilization process is the enzymes can be reused. The re-usability performance of urease immobilized PVA/Chitosan nanofibers was determined by 30 activity determinations under optimum conditions. As shown in Figure 10, immobilized urease retained its activity by 85% after 10 uses and 45% after 20 uses. After 30 uses, it lost all of its activity. The results of the reusability of the presented study were compared with the literature data in Table 4.

**Table 3.** The kinetic parameters of free and immobilized urease.

	$K_m$ (mM)	$V_{max}$ ( $\mu\text{mol NH}_3/\text{dk}^{-1}$ )
Free urease	0.177	0.369
Urease immobilized PVA/Chitosan nanofiber	0.181	0.306

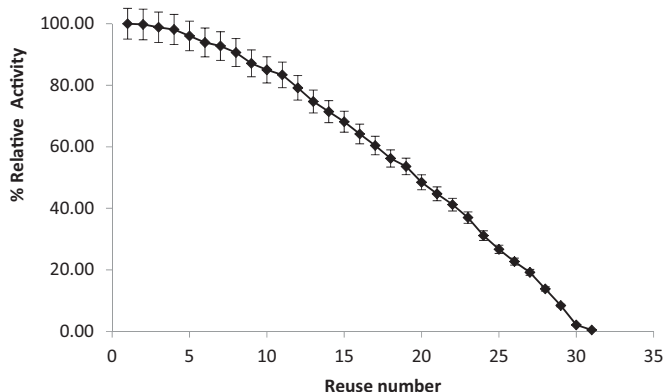


**Figure 10.** Re-usability profile of urease immobilized PVA/Chitosan nanofibers (0.75 mg/mL urease amount, 15 mg fiber amount, 30 min adsorption time, 20  $\mu\text{L}$  GA).

### Recycled reactor design with urease immobilized PVA/chitosan nanofibers for urea removal from artificial blood serum

Recycled reactor enzyme systems ensure optimum reaction conditions remain constant and control of the reaction. In order to investigate the urea removal performance from artificial blood serum of urease immobilized PVA/Chitosan nanofibers were used recycled reactor system. As shown in Figure 11, time-dependent urea concentrations of each cycle were given. At the end of the first cycle (210 min), urea was completely removed. Urea removal rates in other cycles were as follows: 95% at 2nd, 3rd and 4th cycles; 85% at the 5th cycle; 76% at the 6th cycle, and 65% in the last three cycles. When the urease immobilized PVA/Chitosan nanofibers were observed, it was observed that the fibers were not changed much during the first 6 cycles and the structure of the nanofibers deformed at the end of the 9th cycle. In a study, the urea removal of urease immobilized polyacrylonitrile hollow fiber systems in the colon system was studied and 0.25 mg/mL urea was destroyed in a 4 hr period.<sup>[72]</sup>

### Conclusions

In this work, we suggested an effective immobilization methods for urease immobilization using electrospun PVA/Chitosan nanofibers. The methods lead to the evaluation of an effective process for removal of urea. After determination of the optimum immobilization conditions of urease onto

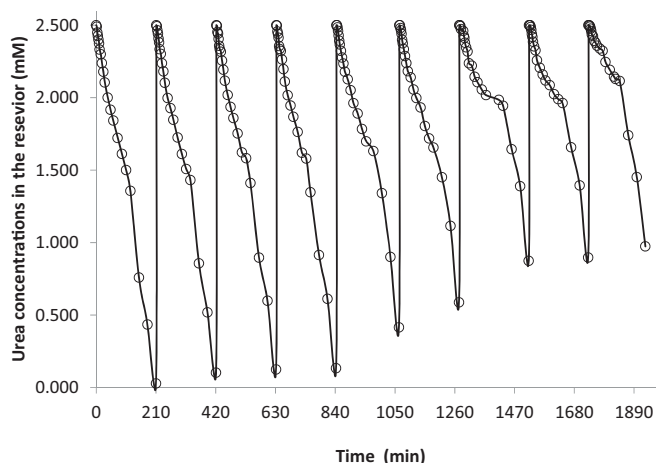


**Figure 11.** Chart of time dependent remaining urea concentration in the reservoir for 9 consecutive cycles.

**Table 4.** The results of the reusability of the presented study were compared with the literature data.

Carrier	Reusability	Reference
Nylon 6/6 tubes	78% activity after 5 uses	[65]
Polyvinyl beads	50% activity after 5 uses	[66]
Alkyl amine glass beads	30% activity after 10 uses	[61]
Arylamine glass beads	18% activity after 10 uses	[61]
Polyaniline membrane 2-hydroxyethyl methacrylate/itaconic acid copolymer	20% activity after 7 uses	[63]
PMIDA-modified $\text{Fe}_3\text{O}_4$ magnetic particles	67% activity after 6 uses	[49]
$\text{TiO}_2$ beads	30% activity after 15 uses	[47]
Electrospun PVA/Chitosan nanofiber	85% activity after 10 uses 70% activity after 15 uses 50% activity after 20 uses	Present study

PVA/Chitosan nanofibers, characteristic properties of immobilized enzyme systems (optimum temperature, optimum pH, kinetic parameters, thermal stability, pH stability, operational stability and reusability) were compared with free urease. We improved the stability properties (especially thermal, pH stability, and reusability) of the urease after immobilization. The criteria of reusability which is extremely important to practical applications were also investigated and activity analysis was performed 30 times in succession. The 50% activity was protected after 20 cycles. The obtained results show clearly that the prepared nanofibers are effective and easily applicable for immobilization of urease.

## Funding

This work was supported by a grant from the Muğla Sıtkı Koçman University Scientific Research Project (Project No:13/182 and 16/038).

## References

- [1] Kartal, F.; Kilinç, A. Immobilization of Pancreatic Lipase on Polyvinyl Alcohol by Cyanuric Chloride. *Prep. Biochem. Biotechnol.* **2006**, *36*, 139–151.
- [2] Caramori, S. S.; Fernandes, K. F. Covalent Immobilisation of Horseradish Peroxidase onto Poly(Ethylene Terephthalate)-Poly(Aniline) Composite. *Proc. Biochem.* **2004**, *39*, 883–888.
- [3] Fernandes, K.; Lima, C.; Lopes, F.; Collins, C. Properties of Horseradish Peroxidase Immobilised onto Polyaniline. *Proc. Biochem.* **2004**, *39*, 957–962.
- [4] Kurokawa, Y.; Sano, T.; Ohta, H.; Nakagawa, Y. Immobilization of Enzyme onto Cellulose-Titanium Oxide Composite Fiber. *Biotechnol. Bioeng.* **1993**, *42*, 394–397.
- [5] Bickerstaff, G. Immobilization of Enzymes and Cells; Humana Press: New York, NY, **1996**; Ed. 1.
- [6] Guncheva, M.; Paunova, K.; Dimitrov, M.; Yancheva, D. Stabilization of *Candida rugosa* Lipase on Nanosized Zirconia-Based Materials. *J. Mol. Catal. B Enzym.* **2014**, *108*, 43–50.
- [7] He, J.; Song, Z.; Ma, H.; Yang, L.; Guo, C. J. Formation of a Mesoporous Bioreactor Based on SBA-15 and Porcine Pancreatic Lipase by Chemical Modification following the Uptake of Enzymes. *J. Mater. Chem.* **2006**, *16*, 4307.
- [8] Foresti, M. L.; Valle, G.; Bonetto, R.; Ferreira, M. L.; Briand, L. E. FTIR, SEM and Fractal Dimension Characterization of Lipase B from *Candida antarctica* Immobilized onto Titania at Selected Conditions. *Appl. Surf. Sci.* **2010**, *256*, 1624–1635.
- [9] Khan, S. A.; Khan, S. B.; Kamal, T.; Asiri, A. M.; Akhtar, K. Recent Development of Chitosan Nanocomposites for Environmental Applications. *Recent Pat. Nanotechnol.* **2016**, *10*, 181–188.
- [10] Chen, Y. W.; Su, Y. L.; Hu, S. H.; Chen, S. Y. Functionalized Graphene Nanocomposites for Enhancing Photothermal Therapy in Tumor Treatment. *Adv. Drug Deliver. Rev.* **2016**, *105*, 190–204.
- [11] Attaran, S. A.; Hassan, A.; Wahit, M. U. J. Materials for Food Packaging Applications Based on Bio-Based Polymer Nanocomposites. *Thermoplast Compos.* **2017**, *30*, 143–173.
- [12] Dogaç, Y. I.; Deveci, I.; Mercimek, B.; Teke, M. *Int. J. Biol. Macromol.* **2017**, *96*, 302–311.
- [13] De Silva, R. T.; Mantilaka, M. M. M. G. P. G.; Ratnayake, S. P.; Amaratunga, G. A. J.; de Silva, K. N. Nano-MgO Reinforced Chitosan Nanocomposites for High Performance Packaging Applications with Improved Mechanical, Thermal and Barrier Properties. *Carbohydr. Polym.* **2017**, *157*, 739–747.
- [14] He, Y.; Yang, S.; Liu, H.; Shao, Q.; Chen, Q.; Lu, C.; Jiang, Y.; Liu, C.; Guo, Z. Reinforced Carbon Fiber Laminates with Oriented Carbon Nanotube Epoxy Nanocomposites: Magnetic Field Assisted Alignment and Cryogenic Temperature Mechanical Properties. *J. Colloid Interf. Sci.* **2018**, *517*, 40–51.
- [15] Wang, C.; Mo, B.; He, Z.; Shao, Q.; Pan, D.; Wujick, E.; Guo, J.; Xie, X.; Xie, X.; Guo, Z. Crosslinked Norbornene Copolymer Anion Exchange Membrane for Fuel Cells. *J. Membrane Sci.* **2018**, *556*, 118–125.
- [16] Cui, X.; Zhu, G.; Pan, Y.; Shao, Q.; Zhao, C.; Dong, M.; Zhang, Y.; Guo, Z. Polydimethylsiloxane-Titania Nanocomposite Coating: Fabrication and Corrosion Resistance. *Polymer.* **2018**, *138*, 203–210.
- [17] Hu, Z.; Shao, Q.; Huang, Y.; Yu, L.; Zhang, D.; Xu, X.; Lin, J.; Liu, H.; Guo, Z. Light Triggered Interfacial Damage Self-Healing of Poly(p-Phenylene Benzobisoxazole) Fiber Composites. *Nanotechnology.* **2018**, *29*, 185602.
- [18] Gu, H.; Zhang, H.; Lin, J.; Shao, Q.; Young, D. P.; Sun, L.; Shen, T. D.; Guo, Z. Large Negative Giant Magnetoresistance at Room Temperature and Electrical Transport in Cobalt Ferrite-Polyaniline Nanocomposites. *Polymer.* **2018**, *143*, 324–330.
- [19] Li, Y.; Zhou, B.; Zheng, G.; Liu, X.; Li, T.; Yan, C.; Cheng, C.; Dai, K.; Liu, C.; Shen, C.; et al. Continuously Prepared Highly Conductive and Stretchable SWNT/MWNT Synergistically Compositing Electrospun Thermoplastic Polyurethane Yarns for Wearable Sensing. *Mater. Chem. C.* **2018**, *6*, 2258–2269.
- [20] Kong, Y.; Li, Y.; Hu, G.; Lin, J.; Pan, D.; Dong, D.; Wujick, E.; Shao, Q.; Wu, M.; Zhao, J.; et al. Preparation of Polystyrene-b-Poly(Ethylene/Propylene)-b-Polystyrene Grafted Glycidyl Methacrylate and Its Compatibility with Recycled Polypropylene/Recycled High Impact Polystyrene Blends. *Polymer.* **2018**, *145*, 232–241.
- [21] Wu, Z.; Cui, H.; Chen, L.; Jiang, D.; Weng, L.; Ma, Y.; Li, X.; Zhang, X.; Liu, H.; Wang, N.; et al. Interfacially Reinforced Unsaturated Polyester Carbon Fiber Composites with a Vinyl Ester-Carbon Nanotubes Sizing Agent. *Compos. Sci. Technol.* **2018**, *164*, 195–203.
- [22] Jia, Y. T.; Gong, J.; Gu, X. H.; Kim, H. Y.; Dong, J.; Shen, X. Y. Fabrication and Characterization of Poly (Vinyl Alcohol)/Chitosan Blend Nanofibers Produced by Electrospinning Method. *Carbohydr. Polym.* **2007**, *67*, 403–409.
- [23] Işık, C.; Arabaci, G.; Doğaç, Y. I.; Deveci, I.; Teke, M. Synthesis and Characterization of Electrospun PVA/Zn<sup>2+</sup> Metal Composite Nanofibers for Lipase Immobilization with Effective Thermal, pH Stabilities and Reusability. *Mater. Sci. Eng. C.* **2019**, *99*, 1226–1235.
- [24] Zdzarta, J.; Meyer, A. S.; Jesionowski, T.; Pinelo, M. A General Overview of Support Materials for Enzyme Immobilization: Characteristics, Properties, Practical Utility. *Catalysts.* **2018**, *8*, 92.
- [25] Liang, H. W.; Guan, Q. F.; Chen, L. F.; Zhu, Z.; Zhang, W. J.; Yu, S. H. Macroscopic-Scale Template Synthesis of Robust Carbonaceous Nanofiber Hydrogels and Aerogels and Their Applications. *Angew. Chem. Int. Ed. Engl.* **2012**, *51*, 5101–5105.
- [26] Garche, J.; Dyer, C. K.; Moseley, P. T.; Ogumi, Z.; Rand, D. A. J.; Scrosati, B. *Encyclopedia of Electrochemical Power Sources*; Newnes, Australia. **2013**.
- [27] Guo, Y.; Xu, G.; Yang, X.; Ruan, K.; Ma, T.; Zhang, Q.; Gu, J.; Wu, Y.; Liu, H.; Guo, Z. Significantly Enhanced and Precisely Modeled Thermal Conductivity in Polyimide Nanocomposites with Chemically Modified Graphene via In Situ Polymerization and Electrospinning-Hot Press Technology. *J. Mater. Chem. C.* **2018**, *6*, 3004–3015.
- [28] Guan, X.; Zheng, G.; Dai, K.; Liu, C.; Yan, X.; Shen, C.; Guo, Z. Carbon Nanotubes-Adsorbed Electrospun PA66 Nanofiber Bundles with Improved Conductivity and Robust Flexibility. *ACS Appl. Mater. Interfaces.* **2016**, *8*, 14150–14159.
- [29] Zhang, L.; Yu, W.; Han, C.; Guo, J.; Zhang, Q.; Xie, H.; Shao, Q.; Sun, Z.; Guo, Z. Large Scaled Synthesis of Hierostructured Electrospun TiO<sub>2</sub>/SnO<sub>2</sub> Nanofibers with an Enhanced



- Photocatalytic Activity. *J. Electrochem. Soc.* **2017**, *164*, H651–H656.
- [30] Noshirvani, N.; Ghanbarzadeh, B.; Fasihi, H.; Almasi, H. Starch–PVA Nanocomposite Film Incorporated with Cellulose Nanocrystals and MMT: A Comparative Study. *Int. J. Food Eng.* **2016**, *12*, 37–48.
- [31] Karimi, A.; Wan Daud, W. M. A. Materials, Preparation, and Characterization of PVA/MMT Nanocomposite Hydrogels: A Review. *Polym. Compos.* **2017**, *38*, 1086–1102.
- [32] Heiba, Z. K.; Mohamed, M. B.; Imam, N. G. Fine-Tune Optical Absorption and Light Emitting Behavior of the CdS/PVA Hybridized Film Nanocomposite. *J. Mol. Struct.* **2017**, *1136*, 321–329.
- [33] Mondal, S.; Madhuri, R.; Sharma, P. K. Electrochemical Sensing of Cyanometallic Compound Using TiO<sub>2</sub>/PVA Nanocomposite-Modified Electrode. *J. Appl. Electrochem.* **2017**, *47*, 75–83.
- [34] Jahan, Z.; Niazi, M. B. K.; Gregersen, Ø. W. Mechanical, Thermal and Swelling Properties of Cellulose Nanocrystals/PVA Nanocomposites Membranes. *J. Ind. Eng. Chem.* **2018**, *57*, 113–124.
- [35] More, S.; Dhokne, R.; Moharil, S. Structural Properties and Temperature Dependence Dielectric Properties of PVA–Al<sub>2</sub>O<sub>3</sub> Composite Thin Films. *Polym. Bull.* **2018**, *75*, 909–923.
- [36] Sarwar, M. S.; Niazi, M. B. K.; Jahan, Z.; Ahmad, T.; Hussain, A. Preparation and Characterization of PVA/Nanocellulose/Ag Nanocomposite Films for Antimicrobial Food Packaging. *Carbohydr. Polym.* **2018**, *184*, 453–464.
- [37] Li, Y.; Jing, T.; Xu, G.; Tian, J.; Dong, M.; Shao, Q.; Wang, B.; Wang, Z.; Zheng, Y.; Yang, C.; et al. 3-D Magnetic Graphene Oxide-Magnetite Poly(Vinyl Alcohol) Nanocomposite Substrates for Immobilizing Enzyme. *Polymer.* **2018**, *149*, 13–22.
- [38] Solikhin, A.; Hadi, Y. S.; Massijaya, M. Y.; Nikmatin, S.; Suzuki, S.; Kojima, Y.; Kobori, H. Properties of poly (vinyl alcohol)/chitosan nanocomposite films reinforced with oil palm empty fruit bunch amorphous lignocellulose nanofibers. *J. Polym. Environ.* **2018**, *26*(8), 3316–3333.
- [39] Amri, C.; Mudasir, M.; Siswanta, D.; Roto, R. In Vitro Hemocompatibility of PVA-Alginate Ester as a Candidate for Hemodialysis Membrane. *Int. J. Biol. Macromol.* **2016**, *82*, 48–53.
- [40] Hamdalla, T. A.; Hanafy, T. A. Optical Properties Studies for PVA/Gd, La, Er or Y Chlorides Based on Structural Modification. *Optik* **2016**, *127*, 878–882.
- [41] Juang, R. S.; Wu, F. C.; Tseng, R. L. Solute Adsorption and Enzyme Immobilization on Chitosan Beads Prepared from Shrimp Shell Wastes. *Bioresour. Technol.* **2001**, *80*, 187–193.
- [42] Krajewska, B. Application of Chitin- and Chitosan-Based Materials for Enzyme Immobilizations: A Review. *Enzyme Microb. Technol.* **2004**, *35*, 126–139.
- [43] Zerger, B. Recent advances in the chemistry of an old enzyme, urease. *Bioorg. Chem.* **1991**, *19*, 116–131.
- [44] Ngo, T. T.; Phan, A. P. H.; Yam, C. F.; Lenhoff, H. M. Interference in Determination of Ammonia with the Hypochlorite-Alkaline Phenol Method of Berthelot. *Anal. Chem.* **1982**, *54*, 46–49.
- [45] Islam, S.; Karim, M. R. Fabrication and Characterization of Poly(Vinyl Alcohol)/Alginate Blend Nanofibers by Electrospinning Method. *Colloid Surf. A.* **2010**, *366*, 135–140.
- [46] Bonino, C. A.; Krebs, M. D.; Saquing, C. D.; Jeong, S. I.; Shear, K. L.; Alsberg, E.; Khan, S. A. Electrospinning Alginate-Based Nanofibers: From Blends to Crosslinked Low Molecular Weight Alginate-Only Systems. *Carbohydr. Polym.* **2011**, *85*, 111–119.
- [47] Paipitak, K.; Pornpra, T.; Mongkotalang, P.; Techitdheer, W.; Pecharapa, W. Characterization of PVA-Chitosan Nanofibers Prepared by Electrospinning. *Procedia Eng.* **2011**, *8*, 101–105.
- [48] Esmaili, A.; Beni, A. A. A Novel Fixed-Bed Reactor Design Incorporating an Electrospun PVA/Chitosan Nanofiber Membrane. *J. Hazard. Mater.* **2014**, *280*, 788–796.
- [49] Gilman, J. W.; VanderHart, D. L.; Kashiwagi, T. Thermal Decomposition Chemistry of Poly (vinyl alcohol). U: Fire and Polymers II Materials and Test for Hazard Prevention. ACS. **1995**, 161–185.
- [50] Tămășan, M.; Simon, V. Thermal and structural characterization of polyvinyl alcohol-kaolinite nanocomposites. *Dig. J. Nanomater. Bios.* **2011**, *6*(3), 1311–1316.
- [51] Yang, Z.; Si, S.; Zhang, C. Study on the Activity and Stability of Urease Immobilized onto Nanoporous Alumina Membranes. *Micropol. Mesopor. Mat.* **2008**, *111*, 359–366.
- [52] Akkaya, A.; Uslan, A. H. Sequential Immobilization of Urease to Glycidyl Methacrylate Grafted Sodium Alginate. *J. Mol. Catal. B-Enzym.* **2010**, *67*, 195–201.
- [53] Nabati, F.; Habibi-Rezaei, M.; Amanlou, M.; Moosavi-Movahedi, A. A. Dioxane Enhanced Immobilization of Urease on Alkyl Modified Nano-Porous Silica Using Reversible Denaturation Approach. *J. Mol. Catal. B-Enzym.* **2011**, *70*, 17–22.
- [54] Akkaya, A. Covalent Immobilization of Urease to Modified Ethyl Cellulose. *Fibers Polym.* **2013**, *14*, 22–27.
- [55] Doğaç, Y. I.; Deveci, I.; Teke, M.; Mercimek, B. TiO<sub>2</sub> Beads and TiO<sub>2</sub>-Chitosan Beads for Urease Immobilization. *Mater. Sci. Eng. C. Mater. Biol. Appl.* **2014**, *42*, 429–435.
- [56] Doğaç, Y. I.; Teke, M. Synthesis and Characterisation of Biocompatible Polymer-Conjugated Magnetic Beads for Enhancement Stability of Urease. *Appl. Biochem. Biotechnol.* **2016**, *179*, 94–110.
- [57] Sahoo, B.; Sahu, S. K.; Pramanik, P. A Novel Method for the Immobilization of Urease on Phosphonate Grafted Iron Oxide Nanoparticle. *J. Mol. Catal. B-Enzym.* **2011**, *69*, 95–102.
- [58] Huang, X. J.; Yu, A. G.; Xu, Z. K. Covalent Immobilization of Lipase from *Candida rugosa* onto Poly(Acrylonitrile-co-2-Hydroxyethyl Methacrylate) Electrospun Fibrous Membranes for Potential Bioreactor Application. *Bioresour. Technol.* **2008**, *99*, 5459–5465.
- [59] Huang, X. J.; Chen, P. C.; Huang, F.; Ou, Y.; Chen, M. R.; Xu, Z. K. Immobilization of *Candida rugosa* Lipase on Electrospun Cellulose Nanofiber Membrane. *J. Mol. Catal. B-Enzym.* **2011**, *70*, 95–100.
- [60] Çevik, E.; Şenel, M.; Abasiyanik, M. F. Immobilization of urease on copper chelated EC-Tri beads and reversible adsorption. *Afr. J. Biotechnol.* **2011**, *10*(34), 6590–6597.
- [61] Monier, M.; El-Sokkary, A. M. A. Modification and Characterization of Cellulosic Cotton Fibers for Efficient Immobilization of Urease. *Int. J. Biol. Macromol.* **2012**, *51*, 18–24.
- [62] Meshram, B. H.; Kondawar, S. B.; Mahajan, A. P.; Mahore, R. P.; Burghate, D. K. Urease Immobilized Polypyrrole/Multi-Walled Carbon Nanotubes Composite Biosensor for Heavy Metal Ions Detection. *J. Chinese Adv. Mater. Soc.* **2014**, *2*, 223–235.
- [63] Doğaç, Y. I.; Teke, M. Immobilization of Bovine Catalase onto Magnetic Nanoparticles. *Prep. Biochem. Biotechnol.* **2013**, *43*, 750–765.
- [64] Bayramoğlu, G.; Altintas, B.; Arica, M. Y. Immobilization of Glucoamylase onto Polyaniline-Grafted Magnetic Hydrogel via Adsorption and Adsorption/Cross-Linking. *Appl. Microbiol. Biotechnol.* **2013**, *97*, 1149–1159.
- [65] Bayramoğlu, G.; Yalçın, E.; Arica, M. Y. Immobilization of Urease via Adsorption onto l-Histidine–Ni(II) Complexed Poly(HEMA-MAH) Microspheres: Preparation and Characterization. *Proc. Biochem.* **2005**, *40*, 3505–3513.
- [66] Yürekli, Y.; Altunkaya, S. A. Catalytic performances of chemically immobilized urease under static and dynamic conditions: A comparative study. *J. Mol. Catal. B-Enzym.* **2011**, *71*(1-2), 36–44.
- [67] Mangaldas, K. S.; Rajput, Y. S.; Sharma, R. Urease Immobilization on Arylamine Glass Beads and Its Characterization. *J. Plant Biochem. Biotechnol.* **2010**, *19*, 73–77.

- [68] Reddy, K. R. C.; Kayastha, A. M. Improved Stability of Urease upon Coupling to Alkylamine and Arylamine Glass and Its Analytical Use. *J. Mol. Catal. B-Enzym.* **2006**, *38*, 104–112.
- [69] Gabrovska, K.; Georgieva, A.; Godjevargova, T.; Stoilova, O.; Manolova, N. Poly(Acrylonitrile)Chitosan Composite Membranes for Urease Immobilization. *J. Biotechnol.* **2007**, *129*, 674–680.
- [70] Hamdy, S. M.; El-Sigeny, S.; Taleb, M. F. A. Immobilization of urease on (HEMA/IA) hydrogel prepared by gamma radiation. *J. Macromol. Sci.* **2008**, *45*(12), 980–987.
- [71] Laska, J.; Włodarczyk, J.; Zaborska, W. Polyaniline as a Support for Urease Immobilization. *J. Mol. Catal. B-Enzym.* **1999**, *6*, 549–553.
- [72] Yang, M. C.; Lin, C. C. Urea Permeation and Hydrolysis through Hollow Fiber Dialyzer Immobilized with Urease. *Biomaterials* **2001**, *22*, 891–896.